COMPARATIVE ANALYSIS OF MULTIPLE FEEDBACK AND SALLEN KEY BAND-PASS FILTERS FOR DEVELOPMENT OF FERRITE BASED HIGH SENSITIVE FLUXGATE SENSOR

Dr. S.D. Yusuf, Dr. I. Umar and Arafat U.H

ABSTRACT

Geomagnetic storms and sub-storms, sudden commencement, and geomagnetic pulsations are a worldwide disturbance of earth's magnetic field which causes significant damage across the world with a single event. Fluxgate sensor is essential in order to predict such occurrence of the major disturbances. In this study, comparative analysis of Multiple Feedback Band-Pass Filter (MFB-BPF) and Sallen Key Band-Pass Filter (SK-BPF) for the implementation of ferrite based high sensitive Fluxgate Sensor (FS) for earth's magnetic field explorations was carried out using Multisim MATLAB. The harmonics responses of the sensing coil output voltage for the designed fluxgate sensor was tested using the designed second-order MFB-BPF and SK-BPF. The prototype single-axis fluxgate sensor was used to obtain 2nd harmonic magnetic field response with Helmholtz coil. Results show that the 2nd harmonics produced the highest amplitudes of 45.61mV at an excitation current of 18.75mA for MFB-BPF and 51.20mV at excitation current of 50.00mA for the SK-BPF respectively. An indication that the core was strongly saturated at the 2nd harmonics and the MFB-BPF performance proved its superiority over the SK-BPF. The MFB-BPF can be adapted for the development of a high sensitive fluxgate sensor which can be used for earth magnetic field exploration.

Index Terms *multiple feedback, sallen key, Helmholtz coil, band pass filter, fluxgate sensor, comparative analysis, magnetic field.*

Reference *to this paper should be made as follows: Dr. S.D. Yusuf, Dr. I. Umar, and Arafat U, (2022), "Comparative Analysis of Multiple Feedback and Sallen Key Band-Pass Filters for Development of Ferrite Based High Sensitive Fluxgate Sensor" Int. J. Electronics Engineering and Applications, Vol. 10, No. 03, pp. 1-14.*

Biographical notes:

Dr. S.D. Yusuf *is currently a Senior Lecturer in the Department of Physics, Nasarawa State University, Keffi, Nigeria. He holds BSc. in Physics in 1999 and MSc. in applied Physics in 2010 from University of Jos, Nigeria. He obtained his Ph.D. in Engineering in 2005 from Seoul National University, South Korea. He has over 65 publications in reputed journals and conferences. His areas of interest include Electronics Circuit Design and Analysis, Telecommunication, and Medical Physics. He is a Member of Nigerian Institute of Physics.*

Dr. I. Umar *is currently an Associate Professor in the Department of Physics, Nasarawa State University, Keffi, Nigeria. He holds BSc. in Physics in 2001 and MSc. in applied Physics in 2007 from University of Jos, Nigeria. He obtained Ph.D. in Physics in 2014 from Nasarawa State University Keffi, Nigeria. He has over 70 publications in reputed journals and conferences. His areas of interest include Electronics Circuit Design and Analysis, Telecommunication, Radiation and Medical Physics. He is a Member of Nigerian Institute of Physics.*

Arafat U.H *completed his HND in Electrical and Electronics Engineering from Federal Polytechnic Nasarawa, Nigeria. He obtained his PGD in Electronics and communication in 2018 and MSc. in Electronics and Communication in 2020 from Nasarawa State University Keffi, Nigeria. Soon after his bachelor, he has served as Export Credit Officer I in Nigerian Export Import Bank, Abuja for over12 years. He is an active researcher in the areas Electronics and Telecommunication.*

I. INTRODUCTION

Frequent observation of earth's magnetic field is important in order to forecast the occurrence of disturbances on the solar terrestrial environment [1]. This disturbance reaches the earth through the magnetosphere and they include abrupt commencement, geomagnetic pulsations, geomagnetic storms, and sub-storms [2]. Geomagnetic storms are universal disturbances of earth's magnetic fields, which can cause substantial damage across the world [3]. Its occurrence can disrupt a functional electrical power supply system and vital space-based sub-structures which may in turn affect the economic sector of a country. The earth has a varying magnetic field which comprised of strained radiation and plasma zones, originally due to the action of the charged substances of the solar rays striking on the field [4, 5]. The maximum magnetic field a sensor can experience in space is about ±60000nT [6]. Due to inadequate data on earth's magnetic field observations, the occurrence of geomagnetic storms remains a mystery. However, fluxgate sensor is contributing to the ongoing quest in explaining some of the difficulties relating to the geomagnetic storm on the solar terrestrial system [7]. Fluxgate sensors are commonly used magnetic field sensors for measuring DC or low frequency AC magnetic field vectors [6]. The desire for the integration of fluxgate sensors used for the detection of magnitude and direction of earth's magnetic field in complex electronic system have increased [8]. Such magnetic field sensors finds their applications in low power mobile devices such as terrestrial and space navigation systems, military detection, craft navigation, medical recognition, modern digital navigation, and non-destructive inspection [9].

Fluxgate sensors have very high sensitivity, spans a wide range from 100 pT to 100 μT [10], low noise, small size, less power consumption, and high temperature stability [11]. The progress in magnetic materials which form the heart of Fluxgate Sensor (FS) and characterizes their sensitivity, noise level, and linearity range is responsible for their popularity among other competitive magnetic field sensors [12]. These makes them one of the magnetic field sensors that still draws the attention of many investigators because of their broad applications [13] in space research and navigation systems [14], especially in Earth's magnetic field exploration surveys [15]. Hence, the objective of this research is to carry out a comparative analysis of Multiple Feedback Band-Pass Filter (MFB-BPF) and Sallen Key Band-Pass Filter (SK-BPF) for the implementation of a ferrite based high sensitive Fluxgate Sensor (FS) using Multisim MATLAB. The harmonics responses of the designed fluxgate sensor will be tested using the designed second-order MFB-BPF and SK-BPF to determine the sensing coil output voltage. Analysis of the magnetic field distribution and excitation current needed to saturate the ferromagnetic core material will be carried out by using electromagnetic software tool. The performance responses of the FS will be evaluated by measuring the sensitivity using the magnetic field of the Helmholtz coils for earth's magnetic field explorations.

2. MATERIALS

The materials used for the simulation and analysis of the ferrite based high sensitive fluxgate sensor and their specifications includes Tektronix TPS 2024B Two Channel Digital Oscilloscope, UT-51 LCR Meter, Tenmars TM-191 Magnetic Field Strength Meter, Tektronix (0-72V, 1.2A) PSW 4721Programmable DC Power Supply, Bar Magnet, Tektronix 2050 Digital Multi-Meter, Agilent N9230B 9KHz -3GHz Spectrum Analyzer, Helmholtz Coils, Analog Magnetic Compass, Dataq Dl-145Data Acquisition Meter, 5kHz Testing Board, WINDAQ Software, Firefly Optimization Algorithm, and Acer Laptop Intel® core™ i5 – 420U 1.7GHz with Turbo Boost up to 2.7GHza.

3. METHOD

The method adapted for the comparative analysis of Multiple Feedback and Sallen Key Band-Pass Filters for development of ferrite based high sensitive Fluxgate Sensor covers software design, and output test analysis.

3.1 SOFTWARE DESIGN

The software design involves simulation of the circuit, flowchart, algorithm and choice of programming language.

A. Circuit Simulation

The simulation of the fluxgate sensor was first done part-by-part, then simulation of the full schematic of the fluxgate sensor was carried out to simultaneously find the excitation coil, sensing coil, and detection circuit behavior that would satisfy the desired design constraints for the fluxgate sensor. Data for the fluxgate sensor stages are displayed on the virtual terminals to show the electrical characteristics as well as the plots for the oscillatory waveform. The simulation was achieved following the block diagram as shown in figure 1.

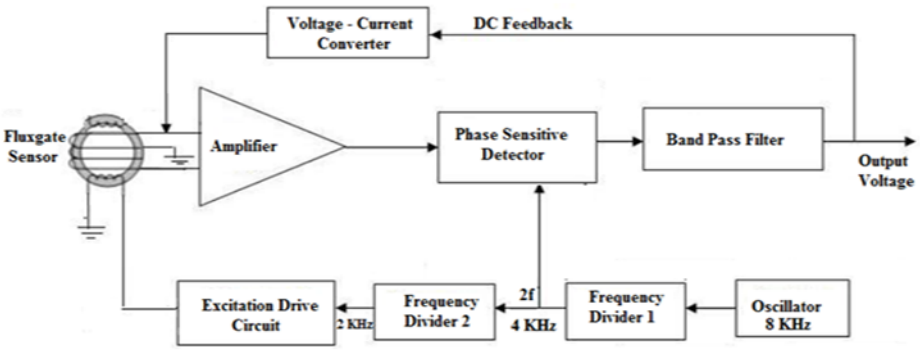

Fig. 1. Block diagram of the Fluxgate Sensor.

B. Flowchart

The Graphic User Interphase GUI method in ANSYS was used to generate the flowchart for the implementation of the Fluxgate Sensor stages. The flowchart of the system is shown in figure 2.

C. Algorithm

The algorithm for the system can be explained as follows:

i. Start
ii. Circuit design
iii. Circuit design validation to ensure the feasibility of the design.
iv. Component selection on the software application.
v. Circuit connection using selected components.
vi. Run simulation
vii. Is the sensor OK? IF YES, then construct, Excite and test the sensor, but
If NO, go back to the circuit design and verify the reason.
viii. Does the result validate the design? If YES, characterize the sensor, but

If NO, go back to the Circuit Design

ix. End.

D. Choice of Programming Language

The programming language choosing for this research work is “Multisim software”, from National Instrument due to its ability to combine SPICE simulation and circuit design in to an environment optimized to simplify common design tasks, which helps in improving performance, minimizes error and shorten time to prototype. Its seamless integration with the ultiboard PCB layout tools makes it easy for one to confidently iterate through design decisions and annotates changes between layouts and circuit schematics.

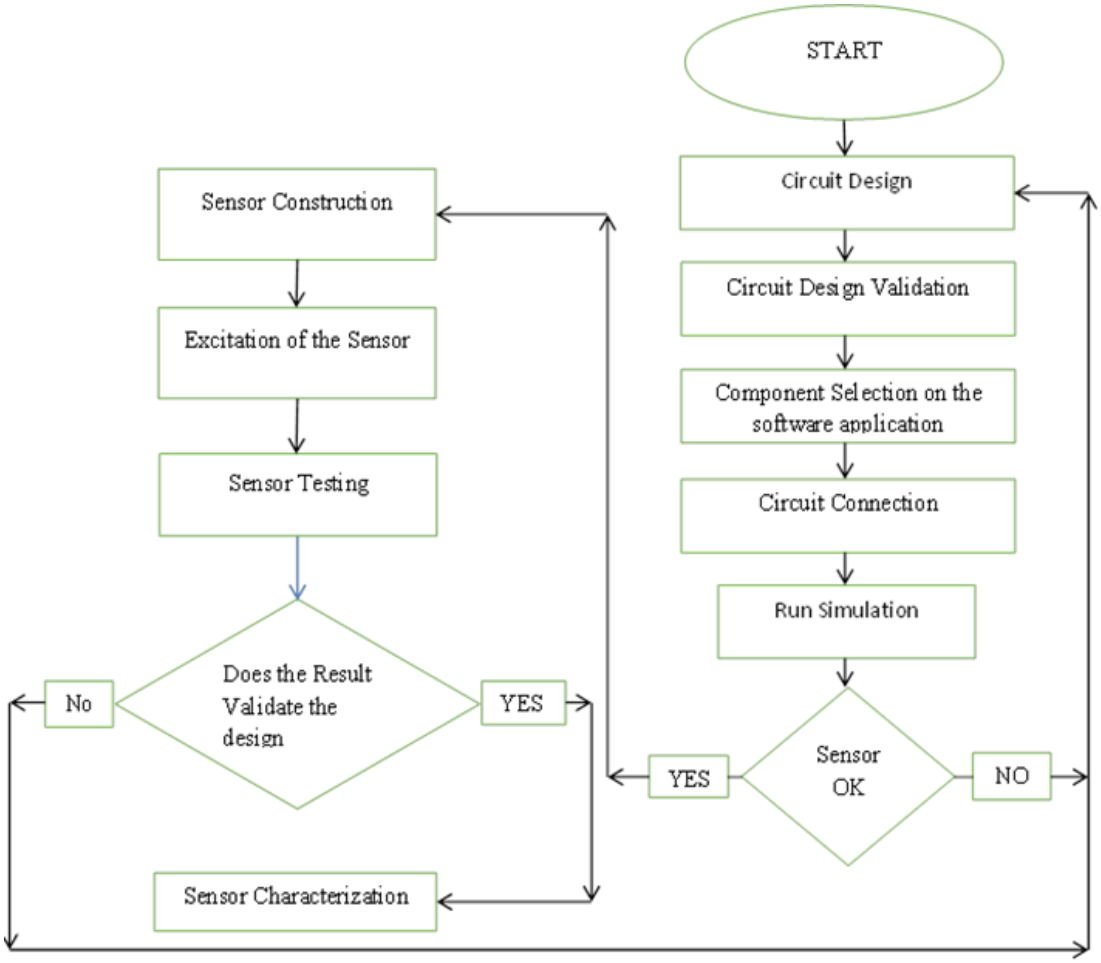

Fig. 2. Flowchart for the proposed Fluxgate Sensor.

3.2 OUTPUT TEST ANALYSIS

The output test analysis was carried out to determine the performance of the simulated circuit as well as to enables us have a proper comparison of the two BPF used in the design. However, the analysis involve carrying out a harmonics response test with MFB-BPF and SK-BPF to monitor the harmonic response patter of the two BPFs. Further analysis with Helmholtz Coil Magnetic Field is also carried out to obtain the best performing filter.

4. RESULTS

4.1 SIMULATION RESULTS

The simulation result for the various output stages are presented in figures 3, 4, 5, 6, and 7 respectively. The simulation result for the complete circuit diagram of the fluxgate sensor is presented in figure 8, while the simulation result of the designed fluxgate sensor with Multiple-Feedback Band Pass Filter and the designed fluxgate sensor with Sellen-Key Band Pass Filter are presented in figures 9 and 10 respectively.

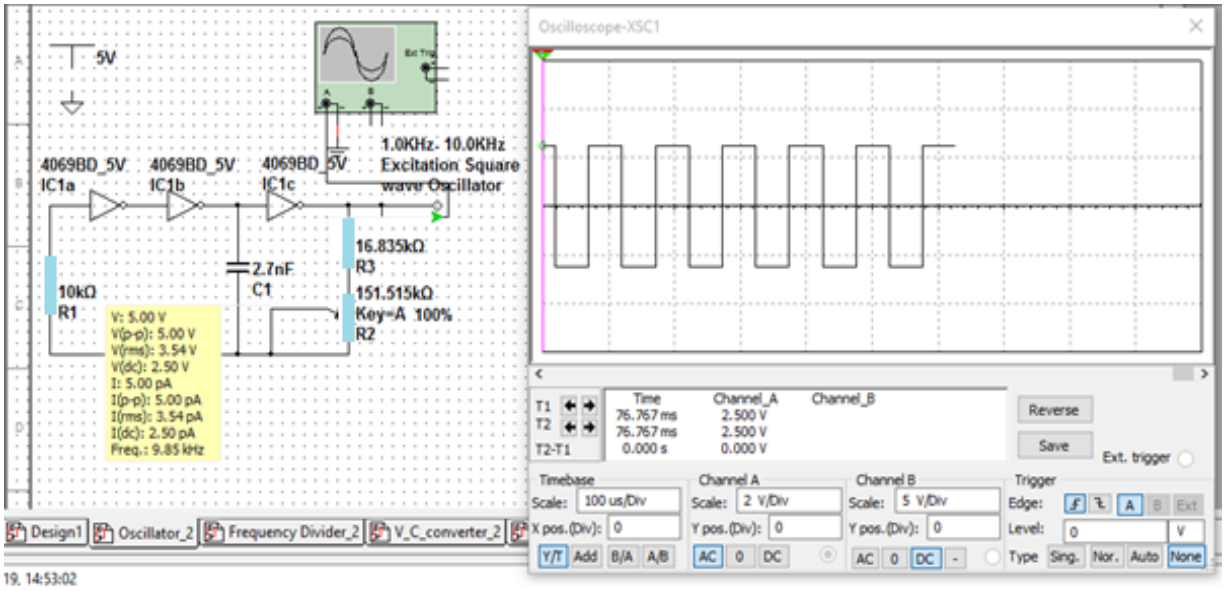

Fig. 3. Simulated frequency generator and waveform from the oscillator stage.

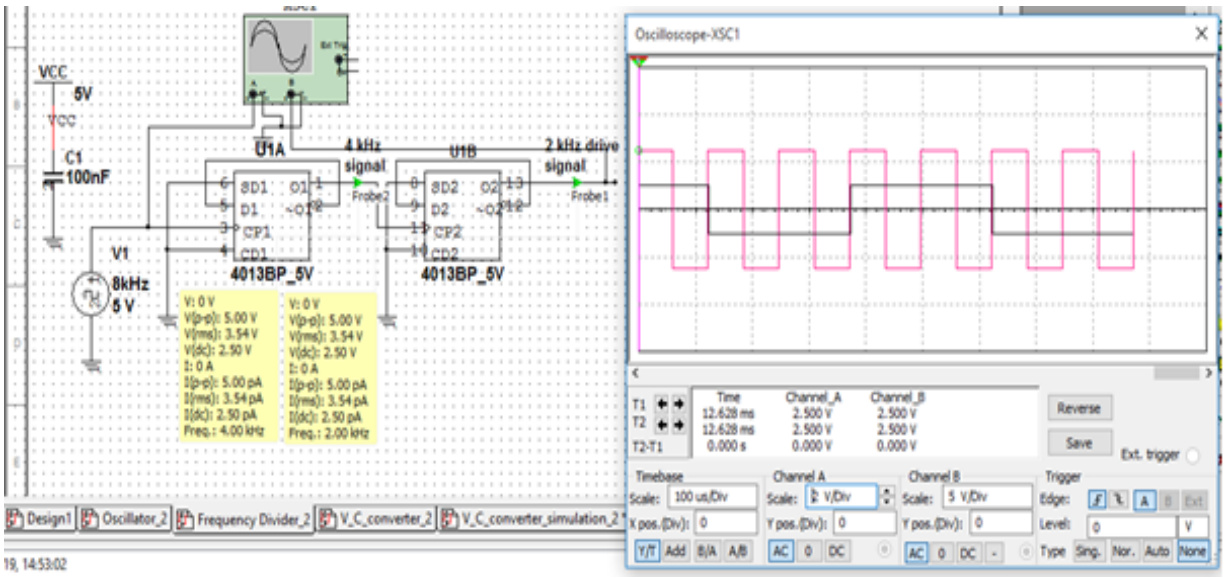

Fig. 4. Simulated frequency divider stage and waveform.

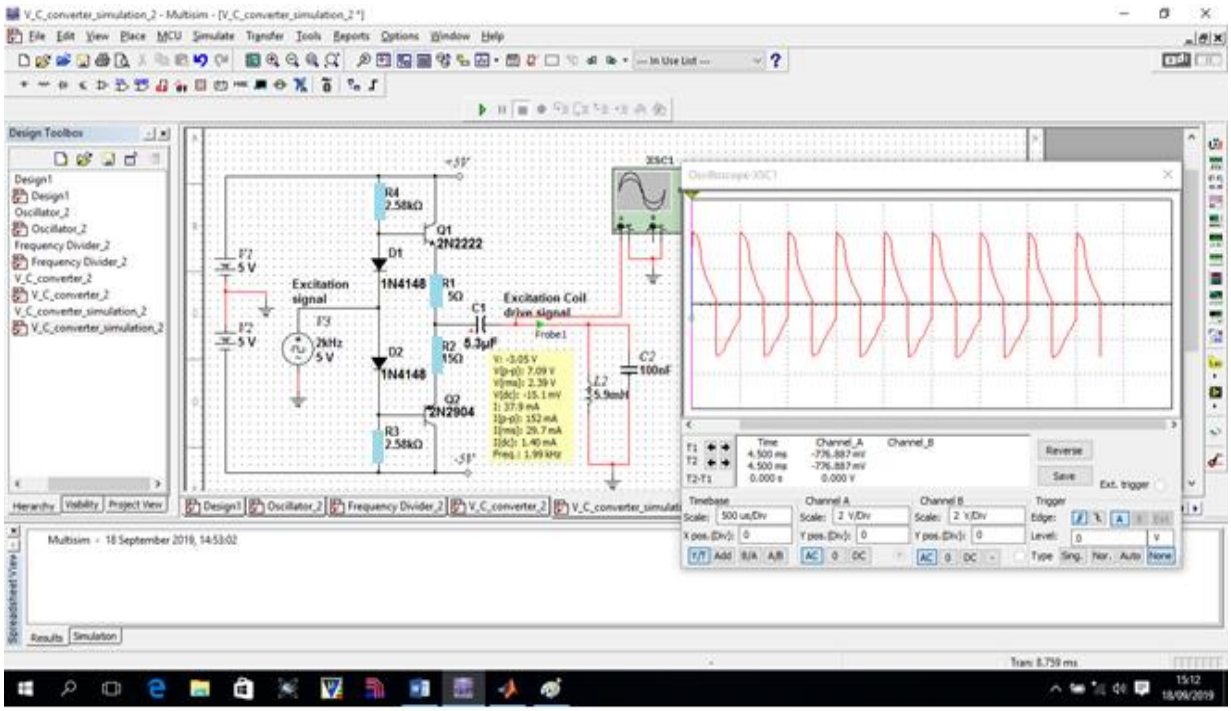

Fig. 5. Simulated voltage to current converter stage and waveform.

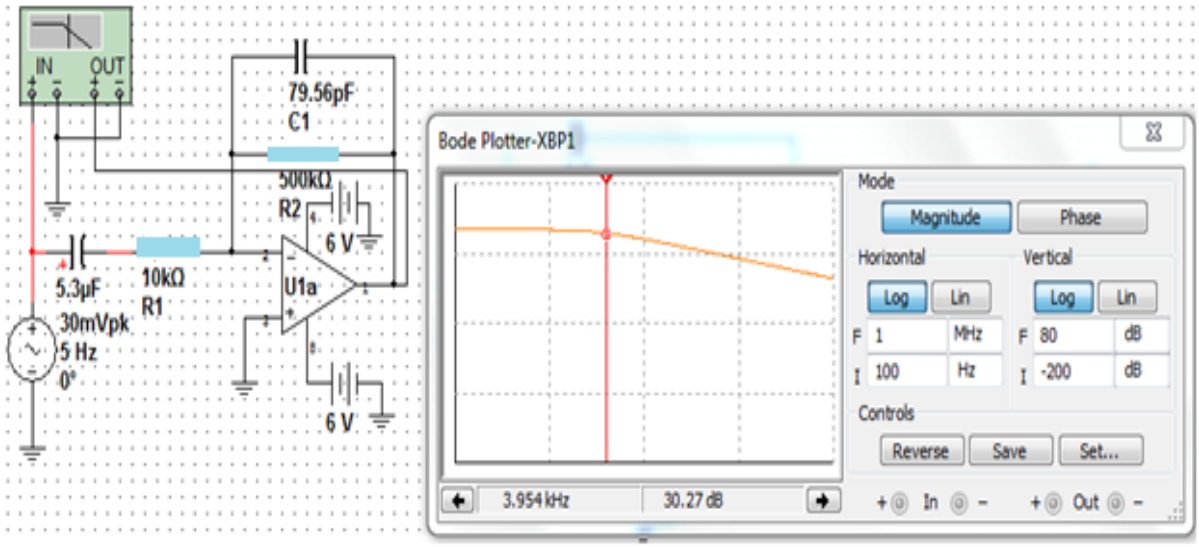

Fig. 6. Simulated current to voltage amplifier stage and waveform.

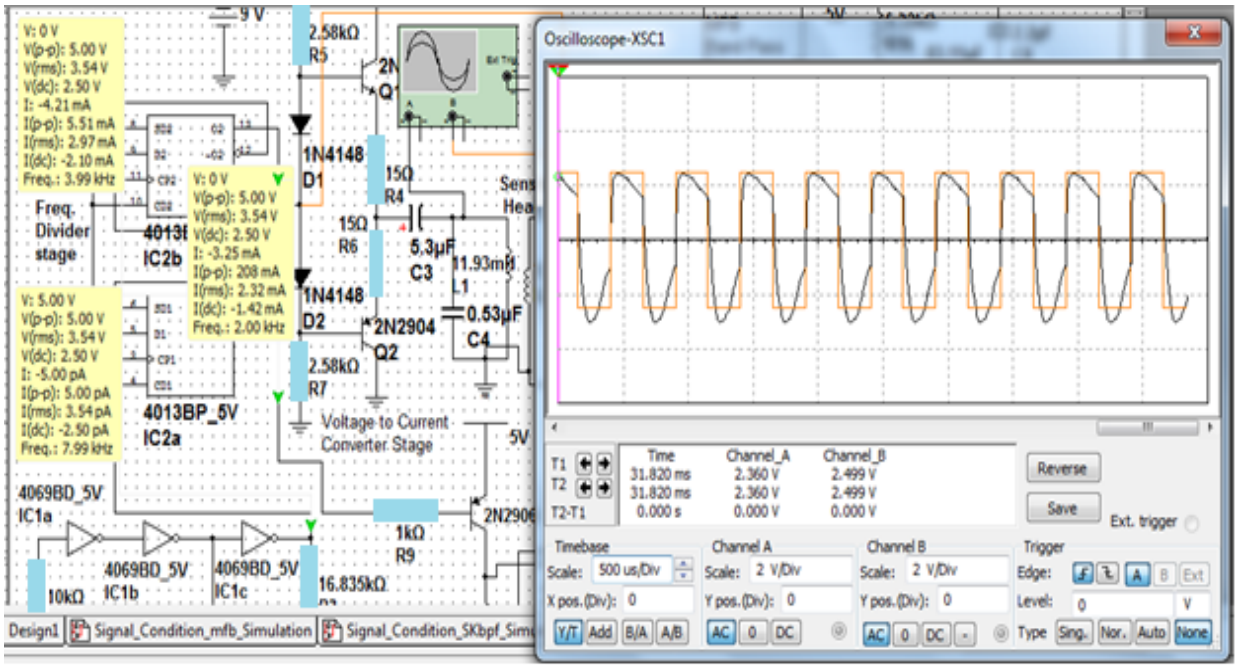

Fig. 7. Simulated excitation stage and waveform.

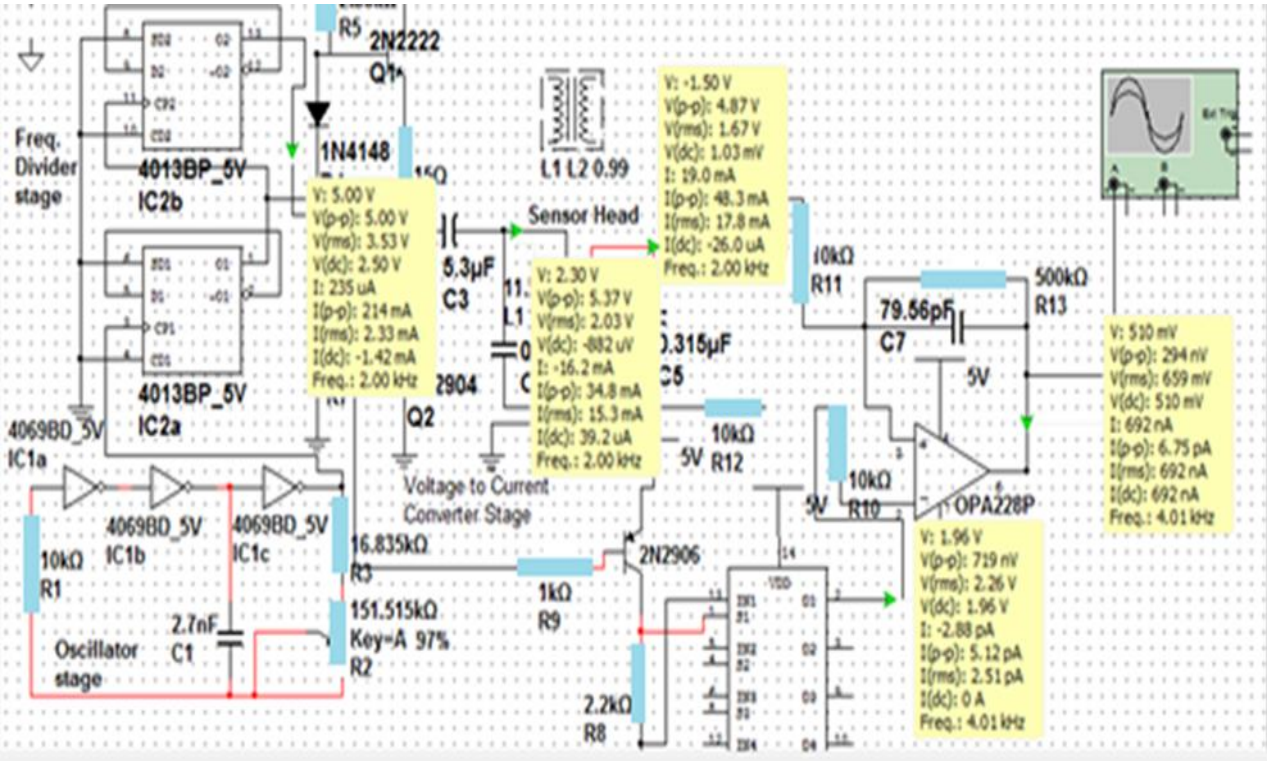

Fig. 8. Simulated full schematic of the designed fluxgate sensor.

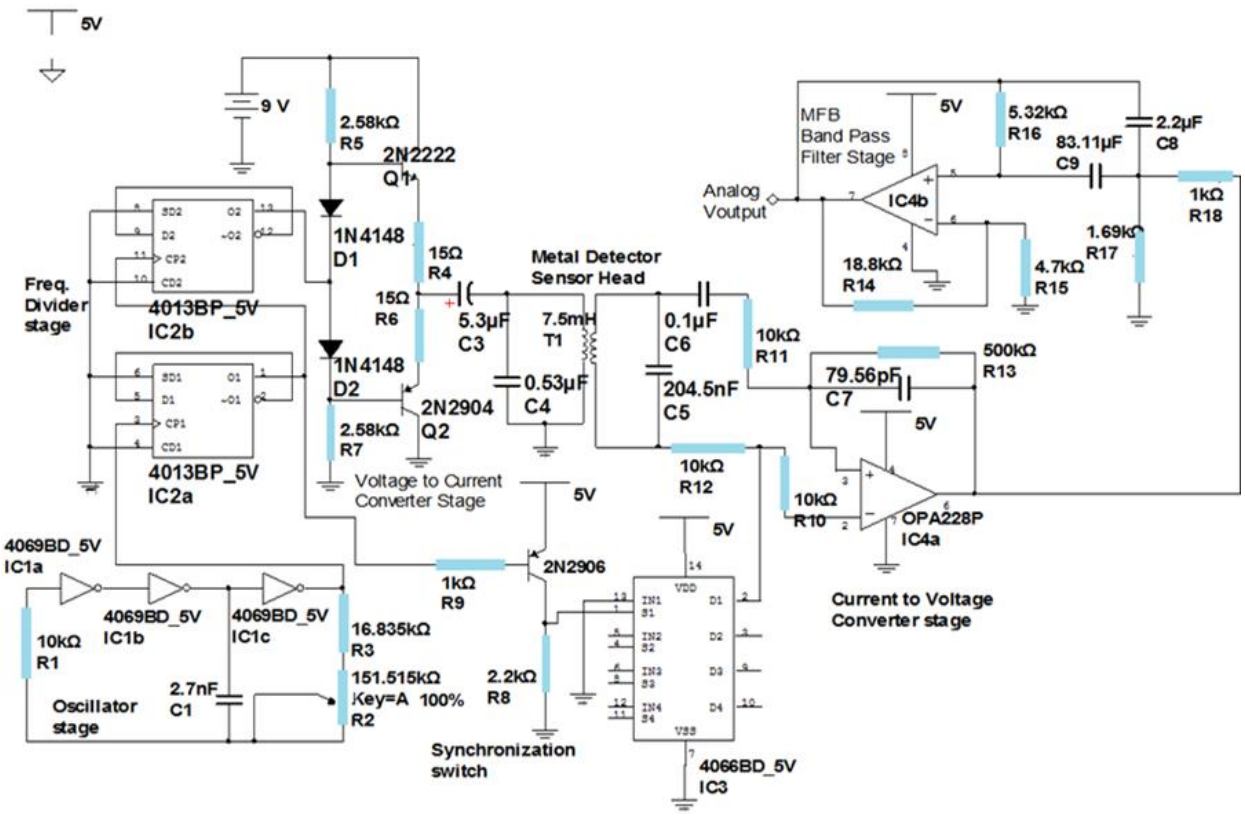

Fig. 9. Complete schematic diagram of the designed FS with MFB-BPF.

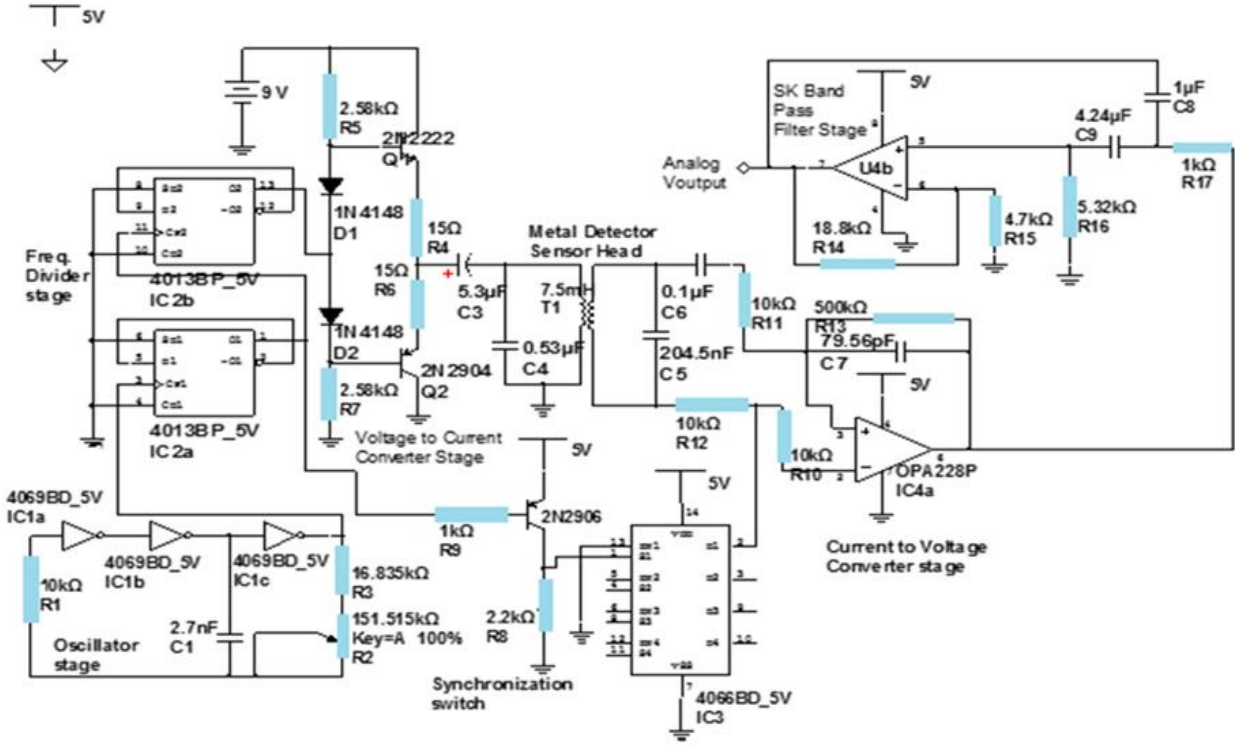

Fig. 10. Complete schematic diagram of the designed FS with SK-BPF.

4.2 OUTPUT TEST ANALYSIS

In order to investigate the harmonics responses of the designed fluxgate sensor using the designed second-order MFB-BPF, the frequency was fixed at 7.07Hz (mid frequency of the BPF) while the excitation current was varied. The amplitude of the fluxgate sensor was measured for 2nd, 3rd, 4th, and 5th harmonics (i.e. 4, 6, 8 and 10kHz) respectively. The sensing coil output voltage responses obtained is presented in Table 1.

Table 1: Harmonic amplitudes of the designed fluxgate sensor with MFB-BPF

Excitation Current (mA)	2nd Harmonic (mV)	3rd Harmonic (mV)	4th Harmonic (mV)	5th Harmonic (mV)
8.33	12.32	8.28	0.29	-
16.66	33.29	12.96	4.08	1.96
18.75	45.61	20.81	11.02	4.81
25.00	43.66	29.29	21.30	13.38
41.66	39.76	31.99	25.16	20.40
50.00	34.97	32.40	26.19	22.93
58.33	32.60	29.19	25.91	23.58
66.66	31.50	27.66	25.38	23.06
75.00	30.27	25.76	25.01	22.68
83.33	28.97	25.05	23.01	22.03
166.66	20.81	19.66	18.85	18.57
250.00	16.97	15.93	15.65	14.44
333.33	14.93	13.90	12.69	11.51
416.66	13.38	12.16	9.55	7.55

With respect to the sensing coil output voltage responses presented in Table I, it is observed that the 2nd harmonic produced the highest amplitude (45.61mV) than other harmonic frequencies at excitation current amplitude of 18.75mA. The result of the different harmonics amplitudes of the sensing coil output for the designed fluxgate sensor with 2nd-Order MFB-BPF is shown in figure 11.

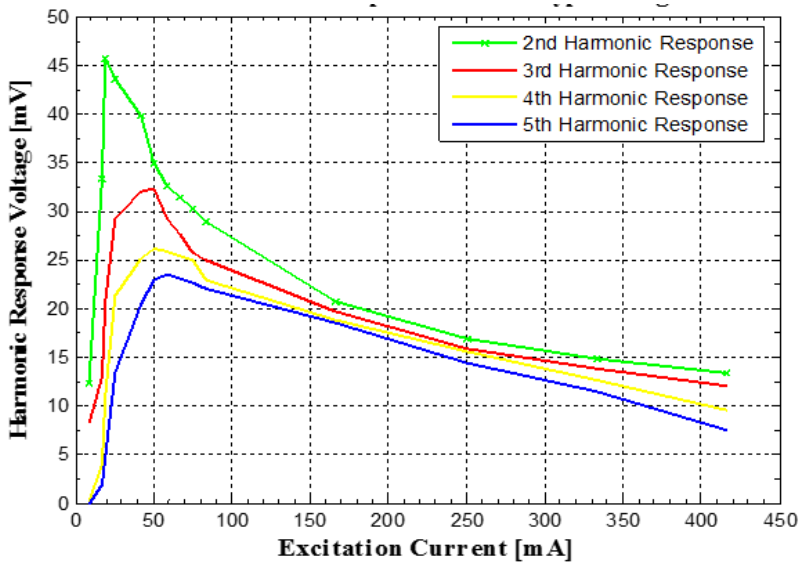

Fig. 11. 2nd-Order MFB-BPF response of prototype fluxgate sensor

The corresponding output waveform shows the optimum performance of each harmonic frequency of the sensing coil output. From fig. 11, it can be seen that the harmonic amplitudes of the sensing coil output signal obtained with MFB-BPF increases with increasing excitation current up to the maximum value, before it starts decreasing with further increase in the excitation current amplitude. In addition, it was further noticed that every harmonic amplitude exhibits a sharp increase until the maximum amplitude is reached, after which a slow decrease started, except for the 2nd and 3rd harmonics which sharply decreases after reaching their peak, then followed by a slow decrease. This behavior demonstrated the attenuation performance of the MFB-BPF.

In order to investigate the harmonics responses of the designed fluxgate sensor using the designed second-order SK-BPF, the frequency was also fixed at 7.07Hz (mid frequency of the BPF) while the excitation current was varied. The same way as MFB, the amplitude of the fluxgate sensor was measured for 2nd, 3rd, 4th, and 5th (i.e. 4, 6, 8, and 10kHz respectively) harmonics of the excitation frequency. The sensing coil output voltage responses obtained is presented in Table 2.

Table 2: Harmonic amplitudes of the developed fluxgate sensor with SK-BPF

Excitation Current (mA)	2nd Harmonic (mV)	3rd Harmonic (mV)	4th Harmonic (mV)	5th Harmonic (mV)
8.33	**6.23**	**10.72**	**0.33**	**0.43**
16.66	**7.51**	**12.91**	**2.20**	**1.19**
18.75	**9.71**	**16.21**	**5.40**	**4.12**
25.00	**14.10**	**22.07**	**15.02**	**8.33**
41.66	**25.83**	**32.52**	**22.90**	**16.30**
50.00	**51.20**	**33.98**	**25.74**	**21.06**
58.33	**49.01**	**35.36**	**26.47**	**23.27**
66.66	**43.51**	**35.91**	**26.11**	**24.09**
75.00	**39.47**	**36.37**	**25.46**	**24.27**
83.33	**38.37**	**36.49**	**24.73**	**23.91**
166.66	**34.35**	**28.72**	**21.16**	**18.78**
250.00	**31.05**	**23.35**	**18.78**	**16.85**
333.33	**28.30**	**20.18**	**16.76**	**15.03**
416.66	**23.83**	**18.56**	**15.02**	**12.66**

With respect to the sensing coil output voltage responses presented in Table 2, it is observed that the 2nd harmonic produced the highest amplitude (51.20mV) than other harmonic frequencies at excitation current of 50mA. The 2nd harmonic amplitude is larger than all other harmonics, which shows that the core is strongly saturated at the second harmonic. The result of the different harmonics amplitudes of the sensing coil output for the designed fluxgate sensor with 2nd-Order SK-BPF is shown in figure 12.

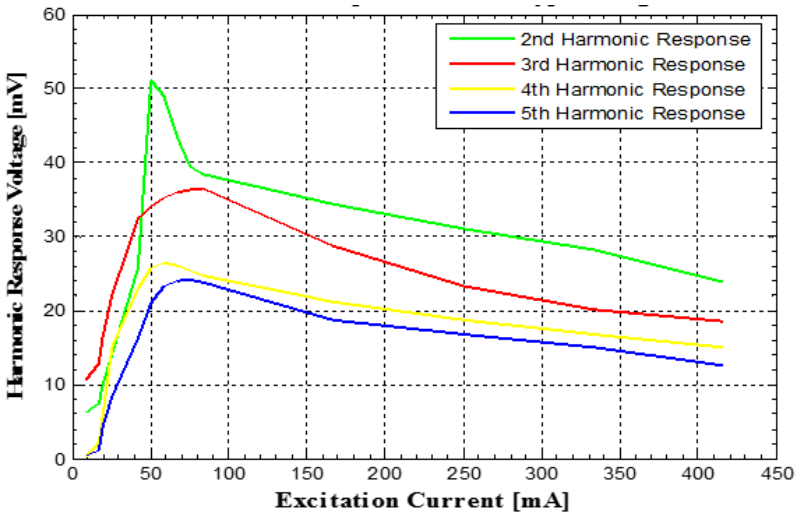

Fig. 12. 2nd-Order SK-BPF response of prototype fluxgate sensor

Again the corresponding output waveform shows the optimum performance of each harmonic frequency of the sensing coil output. From fig. 12, it can also be seen that the harmonic amplitudes of the sensing coil output signal obtained with SK-BPF increases with increasing excitation current up to the maximum value, before it started decreasing with further increase in the excitation current amplitude. Again, it was further noticed that every harmonic amplitudes exhibits a sharp increase until the maximum amplitude is reached, after which a slow decrease started, except for the 2nd harmonic which sharply decreases after reaching its peak, then followed by a slow decrease. This behavior demonstrated the attenuation performance of the SK-BPF.

In order to evaluate the performance of the designed SK-BPF and MFB-BPF along with the fluxgate sensor in this research, the prototype single-axis fluxgate sensor was used to collect 2nd harmonic magnetic field data from Helmholtz coil. The magnetic field between 10µT and 100µT range was been used for the magnetic field characterization of the sensor. The result is presented in Table 3.

Table 3: 2nd harmonic response of the designed FS with Helmholtz coil magnetic field

Helmholtz Coil Magnetic Field (µT)	MFB 2nd Harmonic response (V)	Sallen-Key 2nd Harmonic response (V)
10	**2.546**	**2.291**
20	**2.587**	**2.328**
30	**2.778**	**2.500**
40	**3.142**	**2.828**
50	**3.450**	**3.005**
60	**3.478**	**3.110**
70	**3.484**	**3.136**
80	**3.485**	**3.137**
90	**3.487**	**3.138**
100	**3.487**	**3.138**

From Table 3, it was observed that, with MFB-BPF, the developed fluxgate sensor sensitivity increases with magnetic field from 10µT up to 60µT when it attains about 3.478V, after which the corresponding sensitivity remains the same due to hysteresis effect. Likewise, with SK-BPF, the developed fluxgate sensor sensitivity increases with magnetic field up to 70µT at the corresponding sensitivity of 3.136V, after which further increase in magnetic field yielded no output voltage

response due to hysteresis effect. The results of the 2nd harmonic response applied to the magnetic field for MFB-BPF and SK-BPF is shown in figure 13.

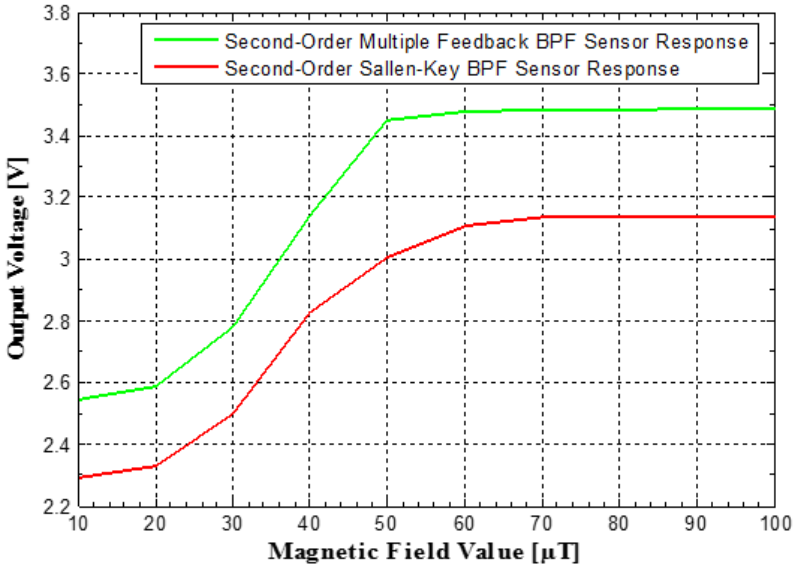

Fig. 13: High magnetic field response of prototype fluxgate sensor

From fig. 13, the corresponding output waveform that shows the optimum performance of the two BPF has revealed vital information for comparison of the two BPF's. Hence, based on the results obtained from the investigations of the two band pass filter configurations, the performance response of the MFB-BPF is better than that of the SK-BPF.

5. DISCUSSION

Findings from this study have revealed that the magnetic core material used was saturated because of the deformed nature of the excitation square waves. This was due to resonance saturation of the ferromagnetic material. As a result, this resonance voltage signal had a strong component at the 2nd harmonic of the excitation frequency because of its capability to attenuate all other unwanted harmonic signals. Accordingly, with MFB-BPF and SK-BPF, the amplitudes of the sensing coil output signal increases with increased in the values of the excitation current up to the maximum, before it started decreasing with further increase in the excitation current value. The sharp increase exhibited by the harmonic amplitudes is the attenuation response of the filter, while the hysteresis curve indicated the saturation of the core. The 2nd harmonic responses for the two BPFs investigated in this research, produced the highest amplitudes as compared to other harmonics i.e. 3rd, 4th, & 5th respectively. This finding is in line with that of [12] who also carried out 2nd harmonic measurements to investigate the sensitivity and noise level in their design of a ring core fluxgate with three different diameters which were prepared by using Metglas 2714A ribbons in traditional 3D wire-wound technology. Also in line with that of [6] who also carried our 2nd harmonic detection to verify V-B relationship and device responsivity in their design of a 3-axis miniature magnetic sensor based on a planar fluxgate magnetometer with an orthogonal fluxguide. Findings from this study have revealed that the 2nd harmonic response for the MFB-BPF was 45.61mV at an excitation current of 18.75mA as compared to that of for the SK-BPF which was 51.20mV at an excitation current of 50.00mV.

This implies that the fluxgate sensor with MFB-BPF consumes less power 0.86W as compared to the fluxgate sensor with SK-BPF 2.56W. This findings is quite different from that of [16] who obtained an excitation current of 31mA at 1.086kHz excitation frequency while implementing a highly sensitive and reliable fluxgate magnetometers for measurement of low frequency AC and DC magnetic field vectors.

Findings from this study have also shown that the linear response of the device to an external applied magnetic field was 60μT at 3.478V and 70μT at 3.136V for the designed fluxgate sensor with MFB-BPF and SK-BPF respectively at 7.07Hz excitation frequency. This finding is quite different from that of [17] who obtained a linear sensor response of ±40μT at 100kHz excitation frequency while working on a flexible flat micro-fluxgate sensor with amorphous rectangular core, using a simple pad-printing technique. Based on the results obtained from the investigations of the two BPF's, the performance response of the MFB-BPF is better than that of the SK-BPF and hence, it adoption for the design and development of the high sensitive fluxgate sensor for earth magnetic field exploration.

6. CONCLUSION

This study carried out a comparative analysis of Multiple Feedback Band-Pass Filter (MFB-BPF) and Sallen Key Band-Pass Filter (SK-BPF) for the implementation of ferrite based high sensitive Fluxgate Sensor (FS) for earth's magnetic field explorations using Multisim MATLAB. The harmonics responses of the sensing coil output voltage of the designed fluxgate sensor was obtained using the designed 2nd order MFB-BPF and SK-BPF. The prototype single-axis fluxgate sensor was used to obtain 2nd harmonic magnetic field response with Helmholtz coil and the results were very appreciable. However, the performance of the fluxgate sensor designed matching the excitation and detection circuits with MFB-BPF proved its superiority over that with SK-BPF in terms of reduced excitation current and the power consumption, higher voltage sensitivity, and high magnetic field response. This indicates that the fluxgate sensor designed with MFB-BPF can be adapted for earth magnetic field exploration.

DECLARATIONS

Acknowledgements: Not applicable

Competing Interests: The authors declare that they have no competing interests.

Funding: This study did not receive any specific grant from funding agencies in the public, commercial, or not-for-profit sectors.

REFERENCES

[1] S.M.E. Yousif, Data Analysis. MAGDAS School, Redeemer's University, Mowe, Ogun State, Nigeria. 2011.

[2] A. Matsuoka, M. Shinohara, Y.M. Tanaka, A. Fujimoto, and K. Iguchi, "Development of fluxgate magnetometers and applications to the space science missions" An Introduction to Space Instrumentation, Vol. 1, Issue 1, 217–225.

[3] W. Baumjohann, "Magnetic field investigation of Mercurys magnetosphere and the inner heliosphere by MMO/MGF" Planet Space Science, Vol. 58, Issue 2, 279–286.

[4] O.T. Waheed, and A. Rehman, "Design and development of a fluxgate magnetometer for small satellites in low earth orbit" Journal of Space Technology, Vol. 1, Issue 1, 78-82.

[5] I.R. Mann, I.J. Rae, L.G. Ozeke, D.M. Miles, and A.W. Yau, Plasma and Radiation in Molniya Orbit (PRIMO) Science Objective and User's Needs Definition Document. Technical report, Universities of Alberta, Edmonton, Canada. 2011.

[6] C.C. Lu, and J. Huang, "A 3-Axis miniature magnetic sensor based on a planar fluxgate magnetometer with an orthogonal fluxguide" Sensors, Vol. 15, Issue 1, 14727-14744.

[7] J. Benkhoff, J.V. Casteren, H. Hayakawa, M. Fujimoto, H. Laakso, M. Novara, P. Ferri, H.R. Middleton, and R. Ziethe, "BepiColombo-Comprehensive exploration of Mercury, Mission overview and science goals" Planet Space Science, Vol. 58, Issue 1, 2–20.

[8] H. Lv, and S. Liu, "Design and fabrication of low power consumption micro fluxgate sensor" Sensors and Transducers, Vol. 182, Issue 11, 22-27.

[9] C.H. Hsieh, C.L. Dai, and M.Z. Yang, "Fabrication and characterization of CMOS-MEMS magnetic micro sensors" Sensors, Vol. 13, Issue 1, 14728-14739.

[10] H. Lv, and S. Liu, "Research on MEMS technology of micro fluxgate sensor" International Journal of Digital Content Technology and its Applications (JDCTA), Vol. 7, Issue 6, 1159-1167.

[11] P. Frydrych, R. Szewczyk, and J. Salach, "Magnetic fluxgate sensor characteristics modeling using extended preisach model" Acta Phys. Pol. A. Vol. 126, Issue 1, 18-19.

[12] H. Can, and U. Topal, "Design of ring core fluxgate magnetometer as attitude control sensor for low and high orbit satellites" Journal of Superconductivity and Novel Magnetism, Vol. 28, Issue 1, 1093-1096.

[13] M.T. Todaro, L. Sileo, and M. De Vittorio, Magnetic field sensors based on micro-electromechanical systems (MEMS) technology. In K. Kevin (2nd Ed.). Magnetic Sensors - Principles and Applications. Europe, Intech Open. Pages 103-124. 2012.

[14] W. Indrasari, M. Djamal, W. Srigutomo, and D. Ramli, "A magnetic distance sensor with high sensitivity based on double secondary coil of fluxgate" IOSR Journal of Applied Physics (IOSR-JAP), Vol. 2, Issue 5, 29-35.

[15] H. Lv, and S. Liu, "Design and fabrication of low power consumption micro fluxgate sensor" Sensors and Transducers, Vol. 182, Issue 11, 22-27.

[16] S. Tanriseven, H. Can, C. Birlikseven, and U. Topal, Highly sensitive Reliable Fluxgate Magnetometer Implementation. https://www.researchgate.net/profile/Sercan-Tanriseven/publication/308846392_A_low_cost_and_simple_fluxgate_magnetometer_implementation/links/5dbb149fa6fdcc2128f5c180/A-low-cost-and-simple-fluxgate-magnetometer-implementation.pdf. (Accessed April 2019).

[17] S. Schoinas, A.M. El Guamra, F. Moreillon, and P. Passeraub, "A Flexible Pad-Printed Fluxgate sensor" Multidisciplinary Digital Publishing Institute Proceedings, Vol. 1, Issue 4, August 2017. https://doi.org/10.3390/proceedings1040615.